

# Dimensional Description of On-line Wear Debris Images for Wear Characterization

WU Tonghai<sup>1,2,\*</sup>, PENG Yeping<sup>1</sup>, DU Ying<sup>1</sup>, and WANG Junqun<sup>1</sup>

*1 Key Laboratory of Modern Design and Rotor Bearing System of Ministry, Xi'an Jiaotong University, Xi'an 710049, China*

*2 School of Mechanical and Manufacturing Engineering, The University of New South Wales, Sydney 2052, Australia*

Received December 19, 2013; revised June 2, 2014; accepted August 8, 2014

**Abstract:** As one of the most wear monitoring indicator, dimensional feature of individual particles has been studied mostly focusing on off-line analytical ferrograph. Recent development in on-line wear monitoring with wear debris images shows that merely wear debris concentration has been extracted from on-line ferrograph images. It remains a bottleneck of obtaining the dimension of on-line particles due to the low resolution, high contamination and particle's chain pattern of an on-line image sample. In this work, statistical dimension of wear debris in on-line ferrograph images is investigated. A two-step procedure is proposed as follows. First, an on-line ferrograph image is decomposed into four component images with different frequencies. By doing this, the size of each component image is reduced by one fourth, which will increase the efficiency of subsequent processing. The low-frequency image is used for extracting the area of wear debris, and the high-frequency image is adopted for extracting contour. Second, a statistical equivalent circle dimension is constructed by equaling the overall wear debris in the image into equivalent circles referring to the extracted total area and perimeter of overall wear debris. The equivalent circle dimension, reflecting the statistical dimension of larger wear debris in an on-line image, is verified by manual measurement. Consequently, two preliminary applications are carried out in gasoline engine bench tests of durability and running-in. Evidently, the equivalent circle dimension, together with the previously developed concentration index, index of particle coverage area (IPCA), show good performances in characterizing engine wear conditions. The proposed dimensional indicator provides a new statistical feature of on-line wear particles for on-line wear monitoring. The new dimensional feature conveys profound information about wear severity.

**Keywords:** wear particle analysis, feature extraction, digital image processing

## 1 Introduction

Wear characterization by ferrographic analysis provides comprehensive insights in diagnosing the wear condition of mechanical system<sup>[1-2]</sup>. Evidently, direct reading and analytical ferrography, widely adopted off-line analysis methods, have played important roles in the early detection of machine faults<sup>[3-6]</sup>. Although the morphological features of wear debris via ferrograph images provided profound understanding of wear mechanism, the real-time wear report for condition-based maintenance remains a challenge for traditional ferrographic analysis<sup>[7]</sup>. Recently, an on-line visual ferrograph (OLVF) sensor presents a feasible approach by providing on-line ferrograph images<sup>[8-9]</sup>. However, the feature extraction from an on-line ferrograph images for wear characterization has been limited due to low resolution and high contamination. Feature extraction has becomes the bottleneck of on-line wear characterization

via the wear debris images.

Wear characterization by quantitative indexes is the foundation for wear analysis. The indexes were categorized into two groups: wear degree and wear mechanism<sup>[10]</sup>. Generally, wear degree was reflected by wear rate, and wear mechanism was reflected by the dimension, color and morphology of wear debris. Many advanced algorithms were investigated for extracting the fine features, such as topography, contour, and color from magnified images of characteristic wear debris<sup>[11-13]</sup>. These algorithms had promoted the intelligent recognition of wear mechanism. However, most algorithms focused on the features of characteristic wear debris selected manually, and the intelligent acquirement of characteristic wear debris was scarcely reported. The difficulty lies in the segmentation of single wear debris from intersecting and overlapping wear debris chains. On the other hand, most algorithms are confined in off-line analysis, and they are not applicable in on-line analysis for two specialties:

First, on-line images have unsatisfied features, such as low magnification, high pollution and wear debris chains<sup>[14-15]</sup>. It was difficult to obtain single wear debris image with high resolution.

\* Corresponding author. E-mail: wt-h@163.com

Supported by the National Natural Science Foundation of China (Grant Nos. 51275381, 50905135), Shaanxi Provincial Science and Technology Planning Project of China (Grant No. 2012GY2-37)

© Chinese Mechanical Engineering Society and Springer-Verlag Berlin Heidelberg 2014

Second, on-line monitoring goes beyond normal protection and it predicts life tendency with consistent and sequence information. The fine features of some specific wear debris contained only the transient information of running process. Hence, the features were effective in fault diagnosis other than monitoring and predication.

In previous works, a new wear characterization has been developed for on-line applications<sup>[10]</sup>. Wear rate was denoted by a statistical concentration index, IPCA (Index of Particle Coverage Area), which was based on the area ratio of wear debris to the whole image<sup>[16-17]</sup>. An equivalent dimensional index of wear debris with on-line images has been constructed<sup>[10]</sup>. Although the equivalent dimensional index performed well in some engineering applications, it was still limited for further applications because its parameters were experience-determined in different situations.

Aiming at on-line wear characterization, a statistical dimension of wear debris was investigated for characterizing the wear mechanism with on-line ferrograph images. The images were processed to extract different geometric information of wear debris efficiently. An equivalent dimensional index was constructed for on-line description. Meanwhile, the validation and the application effect of the developed indexes were examined for on-line wear characterization.

## 2 Decomposition of On-line Ferrograph Image Based on Wavelet

### 2.1 Principle of on-line ferrograph images

The on-line ferrograph system has been applied in many industries with the typical principle as shown in Fig. 1<sup>[9]</sup>. The sensor is fixed on the oil out pipe. The lubricant flows from the oil out pipe into the flow channel. The wear debris carried by the lubricant is deposited under the activated magnetic force. The images of the transmitted light are sequentially captured by the CMOS unit and then transmitted to the computer. Afterwards, the magnetic force is released and the wear debris in the flow channel is flushed away through the oil return pipe. This process is repeated periodically according to the above sequence by instructions. In this way, an automatic on-line oil monitoring is realized.

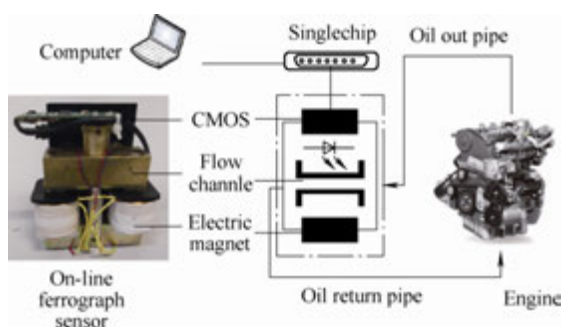


Fig. 1. Schematic diagram of on-line visual ferrograph system

A typical on-line ferrograph image and its gray result are shown in Fig. 2. The bright zone in the image is the objective zone, and the dark strips are wear debris chains. In contrast, off-line image shows the magnified details of single wear debris, and the on-line image shows the coarse contour and shape of wear debris chains. Furthermore, the off-line analysis reports the past wear by manually identifying the magnified images experimentally<sup>[18]</sup>, whereas the on-line analysis identifies the real-time wear by processing the on-line images with rapid and efficient algorithms. In general, the analysis of on-line images should have some particularities<sup>[19]</sup>:

(1) It is difficult and time-consuming to isolate single wear debris from chains. Therefore, a rapid algorithm with focus on overall wear debris is necessary.

(2) The dimension of wear debris distributes in a wide range. A statistical description is more feasible than an accurate one.

(3) On-line monitoring can acquire larger samples in a time span, which is suitable for trend analysis.

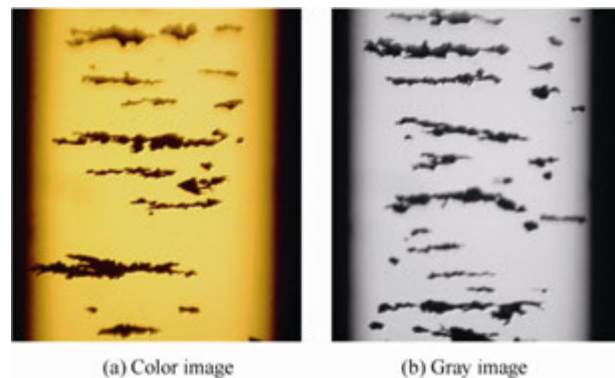


Fig. 2. On-line wear debris image under transmitting light condition

### 2.2 Wavelet-based decomposition

For a gray image, as shown in Fig. 2(b), the boundary of wear debris can be clearly identified from the background by the striking contrast of their gray values. In view of signal processing, a transient variation of the gray values is high frequency information and the similar parts are low frequency information. The decomposition of different frequency information would facilitate the feature extraction.

Wavelets are widely used in image decomposition by frequency analysis. It could extract not only the overall information but also transient details. Time-frequency characteristic of wavelet has been widely adopted in the image identification of faces, flowers, and mountains. A Daubechies wavelet has good orthogonality which ensures complete information about object data. Compared with the Haar wavelet<sup>[20-21]</sup>, the second Daubechies is more suitable for image decomposition<sup>[22]</sup>.

A second Daubechies wavelet was used to decompose the on-line ferrograph image in Fig. 2. The decomposition

results with four component images are illustrated in Fig. 3. The components of low and high frequency are in Fig. 3(a) and Fig. 3(d), and the horizontal and vertical components in Fig. 3(b) and Fig. 3(c), respectively.

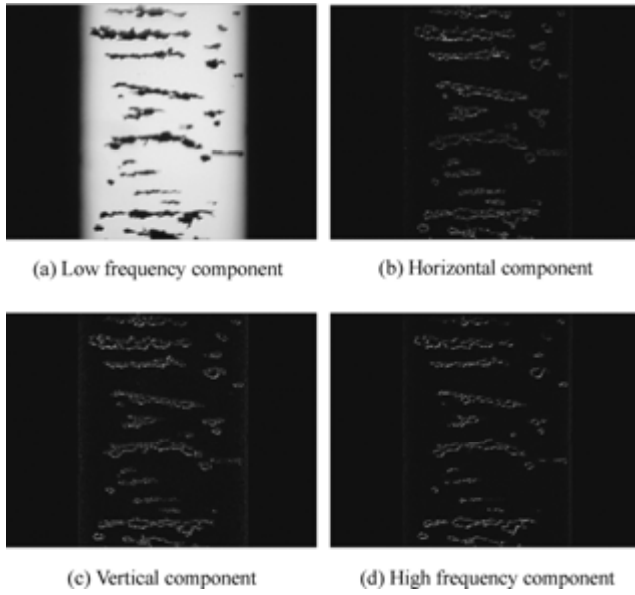


Fig. 3. Wavelet decomposition results of the image in Fig. 2

By comparing the initial image, it was found that most of the boundary pixels of wear debris were well kept in high frequency component, as shown in Fig. 3(d) and residual information of wear debris was kept in the low frequency component, as shown in Fig. 3(a). The area of wear debris could be extracted from a low frequency component image and the contour information from a high frequency one. In addition, the data size of the object image (BMP format) for processing was dramatically reduced by 1/4, which greatly reduced the storage space and transfer rate in the long-term oil monitoring. Moreover, high efficiency could be achieved by using component images.

### 3 Equivalent Dimension of Wear Debris

The dimension of single wear debris has been acquired by identifying the exact contours with high resolution images<sup>[23–25]</sup>. The statistical dimension of wear debris in an on-line ferrograph image was the focus of this work.

#### 3.1 Constructing equivalent dimensional factor

As shown in Fig. 3(d), the contour of each wear debris can be identified by bright pixels from the background. The sum of the bright pixels is equal to the sum of the circumference of overall wear debris which is determined by each circumference and the number of wear debris.

Suppose that a high frequency component image, which is extracted from an  $m \times n$  ( $m$  and  $n$  are the pixels number in the length and width of an image, respectively) on-line gray ferrograph image, is denoted by  $h(x, y)$ , where  $x=1, 2, \dots, m$ ;  $y=1, 2, \dots, n$ ;  $h(x, y) > 0$ . There are only background and wear debris in a gray image, so a binary image is more

suitable for the following process. The binary image can be denoted as

$$g(x, y) = \begin{cases} 0, & h(x, y) > 0, \\ 1, & h(x, y) = 0, \end{cases} \quad (1)$$

where  $g(x, y)$  is the high frequency component of the binary image; 0 denotes the black pixel of the binary image, and 1 denotes the white pixel of the binary image.

As described above, the sum of circumference of overall wear debris,  $M$ , can be defined as

$$M = \sum_{x=1}^m \sum_{y=1}^n g(x, y). \quad (2)$$

To simplify, every wear debris or chain is equivalent to a circle with the same radius,  $R$ . The equivalent circle provides the variables of  $N$  and  $I$ , which are the number and the area of overall wear debris and can be calculated respectively as:

$$M = 2\pi R \times N, \quad (3)$$

$$I = \pi R^2 \times N. \quad (4)$$

Combining Eqs. (3) and (4), we can get the radius of an equivalent circle denoted by:

$$R = \frac{2I}{M}. \quad (5)$$

Therefore, radius of the equivalent circle is correlated with the area and the circumference of overall wear debris. Additionally, the area of overall wear debris can be calculated with the method discussed in Ref. [9].

The dimensional variable  $R$ , calculated by Eqs. (3)–(5), represents the number of pixels. To correlated image pixels with physical dimension, a scale factor  $\lambda$ , is introduced. Thus  $R$  can be rewritten into

$$R = \frac{2\lambda I}{M}. \quad (6)$$

#### 3.2 Principle of the equivalent dimension factor

Consider an on-line image with  $n$  wear debris. Each wear debris chain is equivalent to a circle. The radii of the equivalent circles,  $R_1, R_2, \dots, R_n$ , satisfy the following condition as

$$0 \leq R_1 \leq R_2 \leq \dots \leq R_n. \quad (7)$$

Suppose that the sum of circumferences of overall wear debris is  $M$ , and the sum of areas of overall wear debris is  $I$ . There are two equivalents as

$$M = 2\pi(R_1 + R_2 + \cdots + R_n), \quad (8)$$

$$I = \pi(R_1^2 + R_2^2 + \cdots + R_n^2). \quad (9)$$

Assume that each radius of the equivalent circles is equal. Then, Eqs. (8) and (9) is rewritten as follows:

$$M = 2\pi R \times n, \quad (10)$$

$$I = \pi R^2 \times n. \quad (11)$$

Obtaining the equivalents by considering Eqs. (8)–(11),  $R$  is expressed as

$$R = \frac{R_1^2 + R_2^2 + \cdots + R_n^2}{R_1 + R_2 + \cdots + R_n}. \quad (12)$$

Let  $\bar{R}$  be the average radius of different equivalent circles and it is denoted by

$$\bar{R} = \frac{R_1 + R_2 + \cdots + R_n}{n}. \quad (13)$$

The radii,  $R_1, R_2, \cdots, R_n$ , of the equivalent circles is denoted as

$$R_i = \bar{R} + \alpha_i, \quad i = 1, 2, \cdots, n, \quad (14)$$

where  $\alpha_i$  is the deviation of the radii of different equivalent circles and meets the condition of

$$\sum_{i=1}^n \alpha_i = 0. \quad (15)$$

Take Eq. (14) into Eq. (12), Eq. (12) can be rewritten as

$$R = \frac{R_1^2 + R_2^2 + \cdots + R_n^2}{R_1 + R_2 + \cdots + R_n} = \frac{(\bar{R} + \alpha_1)^2 + (\bar{R} + \alpha_2)^2 + \cdots + (\bar{R} + \alpha_n)^2}{n \cdot \bar{R}}. \quad (16)$$

The variance of deviations is defined as  $\sigma^2$  and denoted by:

$$\sigma^2 = \frac{\alpha_1^2 + \alpha_2^2 + \cdots + \alpha_n^2}{n}. \quad (17)$$

Take Eq. (17) into Eq. (16), the Eq. (16) can be rewritten as

$$R = \bar{R} + \frac{\sigma^2}{\bar{R}}. \quad (18)$$

Then we get

$$R \geq \bar{R}. \quad (19)$$

Considering  $R_1^2 + R_2^2 + \cdots + R_n^2 \leq (R_1 + R_2 + \cdots + R_n)R_n$ , we get

$$R_n \geq \frac{R_1^2 + R_2^2 + \cdots + R_n^2}{R_1 + R_2 + \cdots + R_n}. \quad (20)$$

Combining Eqs. (16), (19) and (20), we get

$$\bar{R} \leq R \leq R_n. \quad (21)$$

The radius of an equivalent circle  $R$  is between the average dimension  $\bar{R}$  and the largest dimension  $R_n$ . It can be drawn from Eq. (18),  $R$  approaches to  $R_n$  as  $\sigma$  increasing. That means the equivalent circle dimension represents larger wear debris when the dimensions of all wear debris becomes more disperse.

### 3.3 Validation of equivalent circle dimension

Three binary on-line ferrograph images were employed for comparison as shown in Fig. 4, respectively. Considering the principle of the equivalent dimension factor, some larger wear debris was marked with numbers. The approximate dimensions of larger wear debris were measured by manually counting pixels. Both the measured and equivalent circle dimensions are shown in Table 1 for validation.

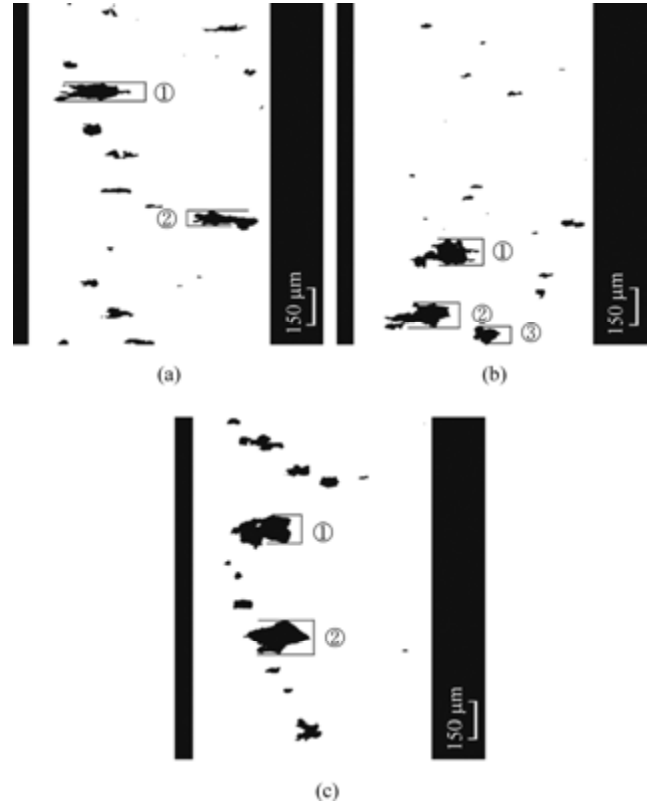


Fig. 4. Binary results of three randomly chosen on-line ferrograph images with marked particles

**Table 1. Comparison of measured and equivalent dimension of selected large wear debris in Fig. 4**

Fig. No.	Particle number	Measured dimension $D/\mu\text{m}$	Equivalent dimension $R/\mu\text{m}$
Fig. 4(a)	①	73.4	68.0
	②	64.9	
Fig. 4(b)	①	98.4	72.1
	②	85.5	
	③	67.5	
Fig. 4(c)	①	113.8	109.9
	②	133.3	

Compared with the manual measurements, the equivalent circle dimensions of the three images were all close to that of larger wear debris. That meant the equivalent circle dimension reflected the statistical dimension of larger wear debris. Accordingly, relative large wear debris often represents transformation from one wear state into another, thus is often focused in wear evaluations. However, the performance of the index in characterizing wear condition still needed to be examined with engineering applications.

#### 4 Engine Application

On-line wear monitoring is very important for most wear-sensitive machines, e.g., engine. Therefore, the method developed in this work was applied in the bench tests of a gasoline engine, which was produced by the Institute of Automotive Engineering of First Automobile Works, commonly known as FAW.

The bench test rig of a gasoline engine and the monitoring system are shown in Fig. 1<sup>[9]</sup>. The tested gasoline engine was mounted on a bench test rig. The output shaft was connected to a dynamometer by a coupler. The on-line oil monitoring system, including an OLVF sensor box and a computer, was placed closely to the test rig. The oil was introduced from the engine's oil tank and then passed through the OLVF sensor. Correspondingly, the images of wear debris were captured and processed by the computer. Then the return oil was sent back to the engine from the oil filter of the engine. On-line images were sampled periodically and automatically during the tests. To characterize wear condition comprehensively, equivalent circle dimension and concentration index, IPCA were calculated from each image.

Two applications were carried out for two typical working conditions. One is the running-in test for about 20 h continuously and the other is the durability test for about 200 h. The experiments were performed and the on-line images were sampled at 2 h intervals.

##### 4.1 Running-in test

The images sampled at different running times during the experiment are given in Fig. 5. The relative concentration of wear debris increased with the running-in process. However, further inspection shows that the number of wear debris chains contributes more to such an increase than that

of larger wear debris. The average dimension of wear debris imperceptibly increased.

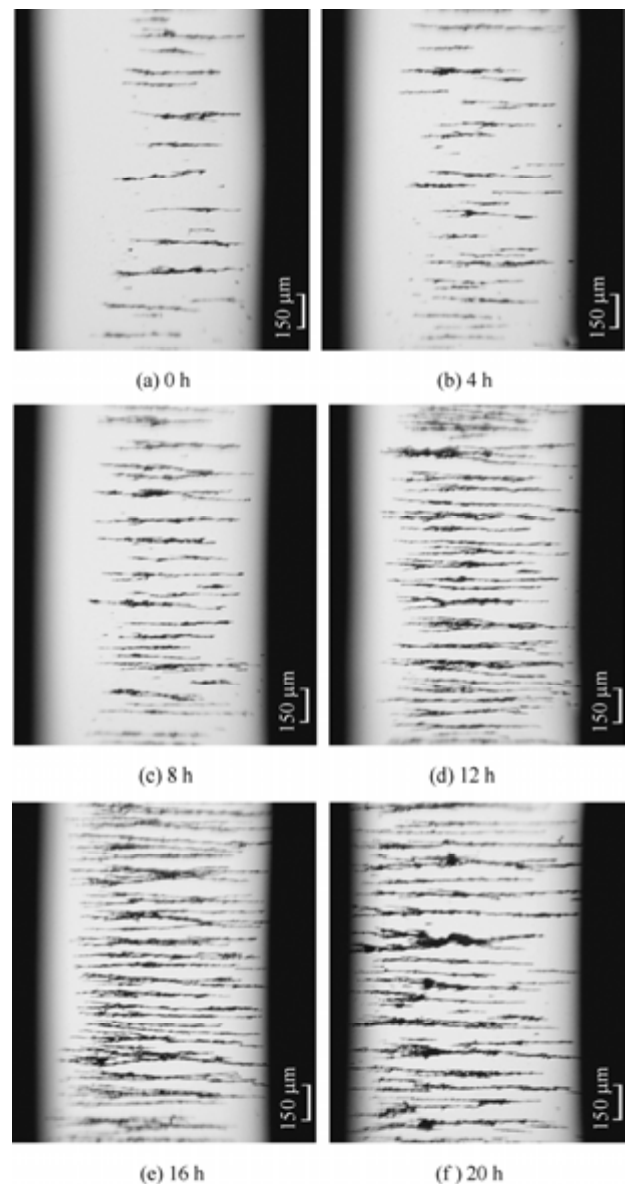


Fig. 5. Images sampled at different running times during running-in bench test for about 20 h

The equivalent circle dimension and the IPCA were calculated from each image and the results were shown in Fig. 6. It was found that the overall trends of the two indexes were not same. The equivalent circle dimension shows slight variation and maintains relative stable average values. By contrast, the IPCA shows an abrupt rate of increase during the running time from 4 h to 12 h and goes up with a gentle rate. The deviation of the two indexes coincides with the intuition fact as can be drawn from Fig. 5.

##### 4.2 Durability test

Images sampled at different running times during the experiment are given in Fig. 7. The relative concentration of wear debris increases during the test. The further inspection shows that the number of small wear debris explicitly increases but the dimension fluctuates slightly.

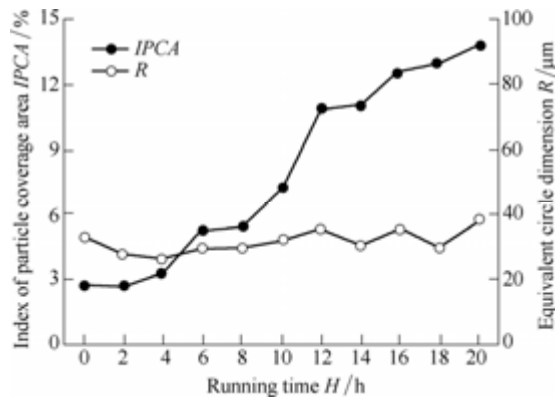


Fig. 6. Variation of the equivalent circle dimension and the IPCA with running time in running-in test of engine

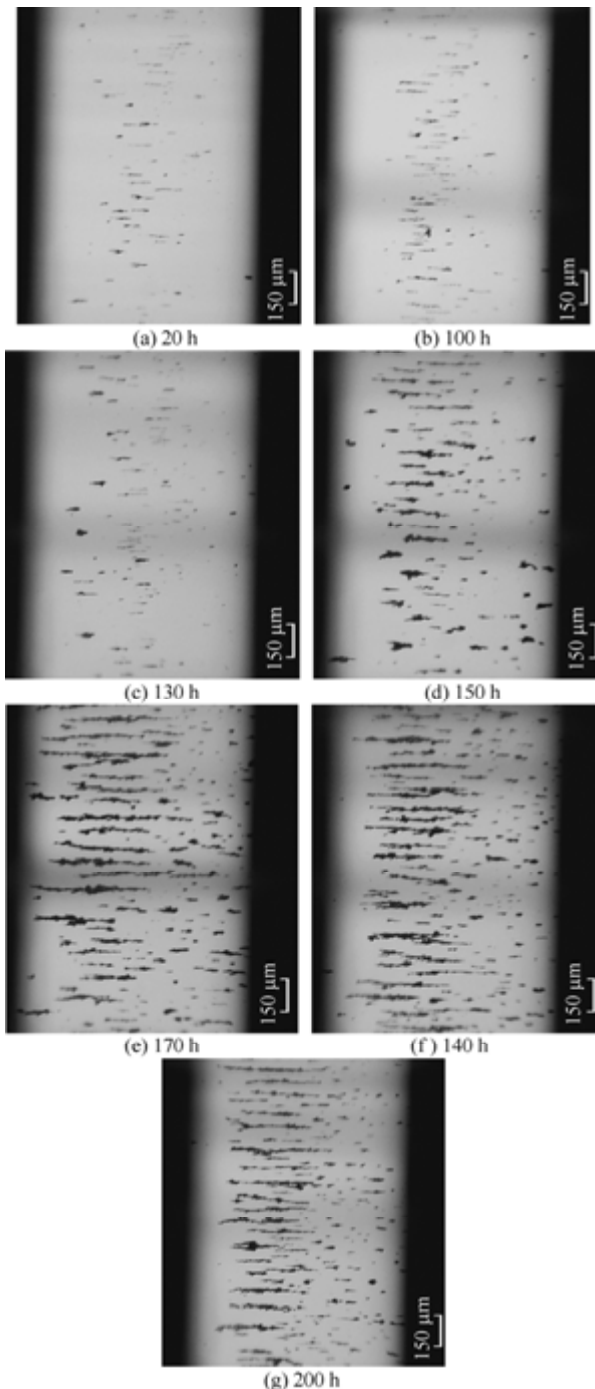


Fig. 7. Part of the images sampled at different running times during durability test for about 200 h

The values of the equivalent circle dimension and IPCA for each image are illustrated in Fig. 8. It can be drawn that the two indexes show similar variations. Two stages of stable wear and severe wear are explicitly exhibited. Absence of the running-in stage in this experiment is because it has been carried out before the test. The dimension and concentration remains stable at the initial stage. A slight fluctuation of the dimension occurred at around 80 h, which reflected the stable wear was deteriorated and large wear debris was produced. Correspondingly, the values of IPCA started a consistent increase after about 100 h, and jumped after about 140 h. In the stable stage, normal wear produced small wear debris and remained a stable wear rate. When the wear station was destroyed, severe wear occurred with larger wear debris and higher wear rate. In addition, the dimension of wear debris remains unvaried in the severe stage but the quantity contributed to the increasing concentration.

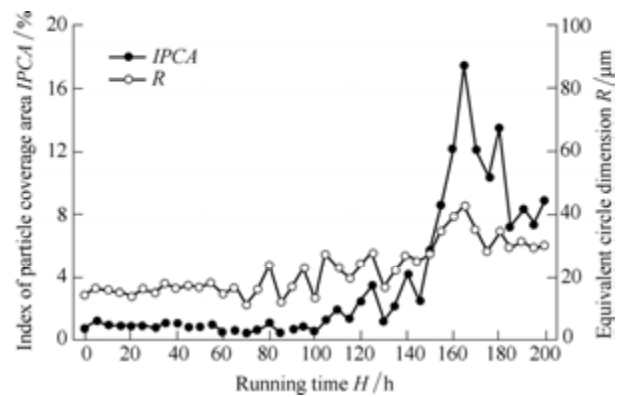


Fig. 8. Variation of the equivalent circle dimension and the IPCA with running time in durability test of engine

As was put forward in the previous study, wear rate and wear mechanism are two independent aspects to characterize the wear condition. In this study, the wear rate represented by the concentration of wear debris and the wear mechanisms represented by equivalent circle dimension well satisfied the principle of the wear processes of engines.

## 5 Conclusions

For on-line wear characterization, a statistical dimension of wear debris was investigated with on-line ferrograph images. An on-line image was decomposed to acquire two frequency component images with different features of wear debris. The statistical features of the two frequency component images were investigated to construct a quantitative index. The validity and the performance of the index were verified by experiments. As a result, some conclusions were generalized as follows.

(1) An equivalent dimension has been constructed to characterize wear mechanism by using the decomposed on-line ferrograph images. Further analysis shows that the index represents the dimension of relative larger wear

debris and satisfies the requirement of abnormal wear detection.

(2) The new index of equivalent circle dimension has a good consistence with the real dimension. Preliminary experiments with the running-in and the durability tests of gasoline engine shows the equivalent circle dimension, together with the wear concentration index, IPCA, can comprehensively characterize wear condition.

## References

- [1] LIU Jin, WANG Jingqiu, WANG Chao. The technical research of ferrography division of morphology[J]. *Advances in Intelligent and Soft Computing*, 2012, 114: 1027–1037.
- [2] ISA M C, YUSOFF N H N, NAIN H, et al. Ferrographic analysis of wear particles of various machinery systems of a commercial marine ship[J]. *Procedia Engineering*, 2013, 68: 345–351.
- [3] MACIAN V, PAYRI R, TORMOS B, et al. Applying analytical ferrography as a technique to detect failures in diesel engine fuel injection systems[J]. *Wear*, 2006, 260(4–5): 562–566.
- [4] MYSHKIN N K, MARKOVA L V, SEMENYUK M S, et al. Wear monitoring based on the analysis of lubricant contamination by optical ferroanalyzer[J]. *Wear*, 2003, 25(7–12): 1270–1275.
- [5] XIAO Hanliang. The development of ferrography in China-some personal reflections[J]. *Tribology International*, 2005, 38(10): 904–907.
- [6] ROYLANCE B J. Ferrography-then and now[J]. *Tribology International*, 2005, 38(10): 857–862.
- [7] LIU Yan, LIU Zhong, XIE Youbai, et al. Research on an on-line wear condition monitoring system for marine diesel engine[J]. *Tribology International*, 2000, 33(12): 829–835.
- [8] WU Tonghai, MAO Junhong, WANG Jingtao, et al. A new on-line visual ferrograph[J]. *Tribology Transaction*, 2009, 52(5): 623–631.
- [9] WU Tonghai, QIU Huipeng, WU Jiaoyi, et al. Image digital processing technology for visual on-line ferrograph sensor[J]. *Chinese Journal of Mechanical Engineering*, 2008, 44(9): 83–87. (in Chinese)
- [10] WU Tonghai, WANG Junqun, WU Jiaoyi, et al. Wear characterization by an on-line ferrograph image[J]. *Proceedings of the Institution of Mechanical Engineers, Part J: Journal of Engineering Tribology*, 2011, 225(1): 23–34.
- [11] CAO Yibo, XIE Xiaopeng. Wear particles classification based on wavelet transform and back-propagation neural network[C]//*Computational Engineering in Systems Applications, IMACS Multiconference on. IEEE*, 2006, 2: 2010–2014.
- [12] RAADNUI S. Wear particle analysis-utilization of quantitative computer image analysis: a review[J]. *Tribology International*, 2005, 38(10): 871–878.
- [13] PODSIADLO P, STACHOWIAK G W. Development of advanced quantitative analysis methods for wear particle characterization and classification to aid tribological system diagnosis[J]. *Tribology International*, 2005, 38(10): 887–897.
- [14] WU Tonghai, WANG Junqun, PENG Yeping, et al. Description of wear debris from online ferrograph images by their statistical color. Tribol[J]. *Tribology Transactions*, 2012, 55(5): 606–614.
- [15] WU Hongkun, WU Tonghai, PENG Yeping, et al. Watershed-based morphological separation of wear debris chains for on-line ferrograph analysis[J]. *Tribology Letters*, 2014, 53(2): 411–420.
- [16] ZHANG Yali, MAO Junhong, XIE Youbai. Engine wear monitoring with OLVF[J]. *Tribology Transactions*, 2011, 54(2): 201–207.
- [17] WU Jiaoyi, MI Xinyan, WU Tonghai. A wavelet-analysis-based differential method for engine wear monitoring via on-line visual ferrograph[J]. *Proceedings of the Institution of Mechanical Engineers, Part J: Journal of Engineering Tribology*, 2013, 227(12): 1356–1366.
- [18] YU Shiqiang, DAI Xingjian. Wear particle image segmentation method based on the recognition of background color[J]. *Tribology*, 2007, 27(5): 467–471. (in Chinese)
- [19] WU Tonghai, WANG Weigang, WU Jiaoyi, et al. Improvement on on-line ferrograph image identification[J]. *Chinese Journal of Mechanical Engineering*, 2010, 23(1): 1–6.
- [20] LI Xianbin, LI Houqiang, WANG Fuqian, et al. A remark on the mallat pyramidal algorithm of wavelet analysis[J]. *Communication in Nonlinear Science & Numerical Simulation*, 1997, 2(4): 240–243.
- [21] MURTAGH F, STARCK J L. Wavelet and curvelet moments for image classification: Application to aggregate mixture grading[J]. *Pattern Recognition Letters*, 2008, 29(10): 1557–1564.
- [22] MRINAL K B, DEBOTOSH B, MITA N, et al. Quotient based multiresolution image fusion of thermal and visual images using daubechies wavelet transform for human face recognition[J]. *International Journal of Computer Science Issues*, 2010, 7(3): 18–22.
- [23] ZHANG G, SCHLARB A K. Morphologies of the wear debris of polyetheretherketone produced under dry sliding conditions: correlation with wear mechanisms[J]. *Wear*, 2009, 266(7–8): 745–752.
- [24] KUMAR M, MUKHERJEE P S, MISRA N M. Advancement and current status of wear debris analysis for machine condition monitoring: a review[J]. *Industrial Lubrication and Tribology*, 2013, 65(1): 3–11.
- [25] GONCALVES V D, ALMEIDA L F, HUGO M. Wear particle classifier system based on an artificial neural network[J]. *Journal of Mechanical Engineering*, 2010, 56(4): 277–281.

## Biographical notes

WU Tonghai, born in 1976, is currently an associate professor at *Theory of Lubrication and Bearing Institute, Key Laboratory of Education Ministry for Modern Design and Rotor-Bearing System, Xi'an Jiaotong University, China*. He obtained his PhD degree from *Xi'an Jiaotong University, China*, in 2006. His research interests include tribology system and intelligent monitoring. Tel: +86-29-82669161; E-mail: wt-h@163.com

PENG Yeping, born in 1988, is currently a PhD candidate at *Theory of Lubrication and Bearing Institute, Key Laboratory of Education Ministry for Modern Design and Rotor-Bearing System, Xi'an Jiaotong University, China*. Her research interests include tribology system and intelligent monitoring. Tel: +86-29-82669161; E-mail: pyp8020@163.com

DU Ying, born in 1989, is currently a PhD candidate at *Theory of Lubrication and Bearing Institute, Key Laboratory of Education Ministry for Modern Design and Rotor-Bearing System, Xi'an Jiaotong University, China*. Her research interests include tribology system and intelligent monitoring. Tel: +86-29-82669161; E-mail: yingdu201007@163.com

WANG Junqun, born in 1985, is currently a MD candidate at *Theory of Lubrication and Bearing Institute, Key Laboratory of Education Ministry for Modern Design and Rotor-Bearing System, Xi'an Jiaotong University, China*. His research interests include tribology system and intelligent monitoring. Tel: +86-29-82669161; E-mail: 594935411@qq.com